SQUEEZE-FILM DAMPERS FOR TURBOMACHINERY STABILIZATION

L. J. McLean and E. J. Hahn
University of New South Wales
Kensington, N.S.W., 2033, Australia

This paper presents a technique for investigating the stability and damping present in centrally preloaded radially symmetric multi-mass flexible rotor bearing systems. In general, one needs to find the eigenvalues of the linearized perturbation equations, though zero frequency stability maps may be found by solving as many simultaneous non-linear equations as there are dampers; and in the case of a single damper, such maps may be found directly, regardless of the number of degrees of freedom. The technique is illustrated for a simple symmetric four degree of freedom flexible rotor with an unpressurized damper. This example shows that whereas zero frequency stability maps are likely to prove to be a simple way to delineate multiple solution possibilities, they do not provide full stability information. Further, particularly for low bearing parameters, the introduction of an unpressurized squeeze film damper may promote instability in an otherwise stable system.

INTRODUCTION

The use of centrally preloaded squeeze film dampers for the attenuation of the unbalance response in turbomachinery has been well documented, and solution techniques which enable all equilibrium operation possibilities to be conveniently portrayed for general multi-degree of freedom rotor bearing systems are increasingly available (refs. 1, 2). However, the question as to which of these equilibrium solutions is stable has not been as fully addressed. Indeed, earlier stability investigations for simpler squeeze film damped flexible rotors (ref. 3) showed that instability (in the linear sense) was indeed possible with unpressurized dampers below and above the first pin pin critical speed, though no instability was noted for pressurized dampers with retainer springs. The utility of squeeze film dampers to accommodate the influence of gyroscopic effects, non-rigid bearing mounts and supercritical operation on stability needs to be better quantified. Hence, it is the purpose of this paper to present a straightforward but general technique for investigating the stability and degree of damping present in general multi-mass flexible rotor bearing systems incorporating one or more centrally preloaded squeeze film dampers. The technique will be illustrated for a simple symmetric four degree of freedom flexible rotor.

SYMBOLS

$\mathbf{A},\mathbf{B}$	square matrices defined by equations (27) and (28)	$\hat{\mathbf{C}}$	$= \mathbf{T}^{-1}\mathbf{C}\mathbf{T}^*$
		$\mathbf{C}^*$	matrix defined by equation (18)
C	radial clearance of damper	C_1	$= c_1/[(m_1+m_2)\omega]$
$\mathbf{C}$	matrix of viscous damping and gyroscopic coefficients	$2c_1$	viscous damping of disc in figure 3

C_{rs}, etc. = $Q_{R34}/[(m_1+m_2)\omega]$, etc.

e_i eccentricity of i^{th} damper; i=1,...,m

$F_{1,2}$ unbalance excitation forces defined by equation (31)

$\underline{F}_S$, $\underline{F}_R$ Vectors of system excitation and hydrodynamic forces in stationary and rotating frames respectively

$\delta\underline{F}_S$, $\delta\underline{F}_R$ vectors of perturbated system excitation and hydrodynamic forces in stationary and rotating frames respectively

F_{S_i}, F_{R_i} elements of $\underline{F}_S$ and $\underline{F}_R$ respectively; i=1,...,n

i subscript (omitted where meaning is clear)

j subscript or $\sqrt{-1}$ depending on context

K system stiffness matrix

K* matrix defined by equation (19)

$K_{1,2}$ = $k_{1,2}/[(m_1+m_2)\omega^2]$

K_{rs}, etc. = $P_{R34}/[(m_1+m_2)\omega^2]$, etc.

k_1 rotor stiffness in figure 3

k_2 retainer spring stiffness in figure 3

L damper length

M system mass matrix

$\hat{\mathbf{M}}$ = $\mathbf{T}^{-1}\mathbf{M}\mathbf{T}^*$

$M_{1,2}$ = $m_{1,2}/[m_1+m_2]$

m number of hydrodynamic damper stations or some characteristic system mass

m matrix defined by equation (A11)

$\hat{\mathbf{m}}$ matrix defined by equation (A12)

$2m_1$ lumped mass of disc in figure 3

m_2 lumped mass at bearing stations in figure 3

n number of system degrees of freedom (necessarily even)

$\mathbf{P}_S$, $\mathbf{P}_R$ matrix of damper stiffness coefficients in stationary and rotating frames respectively

$P_{S_{ij}}$, $P_{R_{ij}}$ elements of $\mathbf{P}_S$ and $\mathbf{P}_R$ defined by equations (7) and (20) respectively

$\mathbf{Q}_S$, $\mathbf{Q}_R$ matrix of damper damping coefficients in stationary and rotating frames respectively

$Q_{S_{ij}}$, $Q_{R_{ij}}$ elements of $\mathbf{Q}_S$ and $\mathbf{Q}_R$ defined by equations (8) and (21) respectively

R radius of damper journal

S, R subscripts denoting stationary (XYZ) and rotating (xyZ) frames respectively

r, s subscripts denoting damper degrees of freedom x_3 and x_4 respectively

T transformation matrix defined by equation (11)

T* matrix defined by equations (A4) to (A6)

t real time

U unbalance parameter = $\rho_1 m_1/[(m_1+m_2)C]$

$\underline{u}$ state vector defined by equation (26)

XYZ, xyZ stationary and rotating cartesian reference frames respectively

$\underline{X}$, $\underline{x}$ system displacement vector in stationary and rotating frames respectively

$\underline{X}_o$, $\underline{x}_o$ system steady state displacement vector in stationary and rotating frames respectively

$\delta\underline{X}$, $\delta\underline{x}$ perturbed system displacement vector in the stationary and rotating frames respectively

X_i, x_i elements of $\underline{X}$ or $\underline{x}$

$\bar{x}_1$, etc. = x_1/C, etc.

γ_i phase difference between i^{th} lumped mass and the stationary frame as defined in figure 2

ε	damper eccentricity ratio = e/C
ζ	damping ratio at rotor mid-span in figure 3 = $c_1/(2m_1\omega_c)$
$\underline{\eta}$	eigenvector of the perturbed system as defined by equation (29)
$\mathbf{A}$	transformation matrix as defined by equation (12)
$\mathbf{A}^*$	matrix defined by equation (A5)
λ	system eigenvalue
μ	lubricant viscosity
ρ_1	disc mass eccentricity in figure 3
τ	non-dimensional time = ωt
ϕ	angle between axes 0X and 0x as defined in figure 2
$\underline{\chi}$	eigenvector of the perturbed system as defined by equation (22)
ψ	Phase difference between rotating and stationary frames as defined in figure 2
Ω	natural frequency at stability threshold
ω	rotor speed
ω_c	a characteristic system frequency = $\sqrt{k_1/m_1}$ in figure 3
ω_b	a bearing parameter = $\mu RL^3/[(m_1+m_2)C^3]$ in figure 3
ω_r	= $\sqrt{k_2/(m_1+m_2)}$
$\dot{}$	denotes differentiation with respect to time t
$'$	denotes differentiation with respect to time τ

THEORY

Figure 1 depicts a general n degree of freedom rotor bearing system incorporating one or more squeeze film dampers. For the system, the equations of motion, in fixed cartesian co-ordinates, may be written as:

$$\mathbf{M}\ddot{\underline{X}} + \mathbf{C}\dot{\underline{X}} + \mathbf{K}\underline{X} = \underline{F}_S(\underline{X},\dot{\underline{X}}) \ . \tag{1}$$

Assuming (i) axially symmetric rotor and foundation stiffnesses, (ii) viscous damping, (iii) central preloading of the hydrodynamic dampers, (iv) synchronous unbalance excitation, (v) negligible torsional and axial vibration, one can obtain circular synchronous solutions $\underline{X}_o$ to equation (1) as explained in reference 2, i.e.

$$\mathbf{M}\ddot{\underline{X}}_o + \mathbf{C}\dot{\underline{X}}_o + \mathbf{K}\underline{X}_o = \underline{F}_S(\underline{X}_o,\dot{\underline{X}}_o) \ . \tag{2}$$

Note that $\underline{X}_o$ is a function of time. It is the degree of stability of these steady state solutions $\underline{X}_o$ that is of interest.

If the steady state solution $\underline{X}_o$ is perturbed by $\delta\underline{X}$ to $\underline{X}$, whereupon $\underline{F}_S(\underline{X}_o,\dot{\underline{X}}_o)$ changes to $\underline{F}_S(\underline{X},\dot{\underline{X}})$, i.e. if:

$$\underline{X} = \underline{X}_o + \delta\underline{X} \ , \tag{3}$$

then substitution of equation (3) in equation (1) and utilizing equation (2) yields:

$$\mathbf{M}\delta\ddot{\underline{X}} + \mathbf{C}\delta\dot{\underline{X}} + \mathbf{K}\delta\underline{X} = \delta\underline{F}_S \ , \tag{4}$$

where

$$\delta\underline{F}_S = \underline{F}_S(\underline{X},\dot{\underline{X}}) - \underline{F}_S(\underline{X}_o,\dot{\underline{X}}_o) \tag{5}$$

$$= \mathbf{P}_S\delta\underline{X} + \mathbf{Q}_S\delta\dot{\underline{X}} + \text{higher order terms} \ , \tag{6}$$

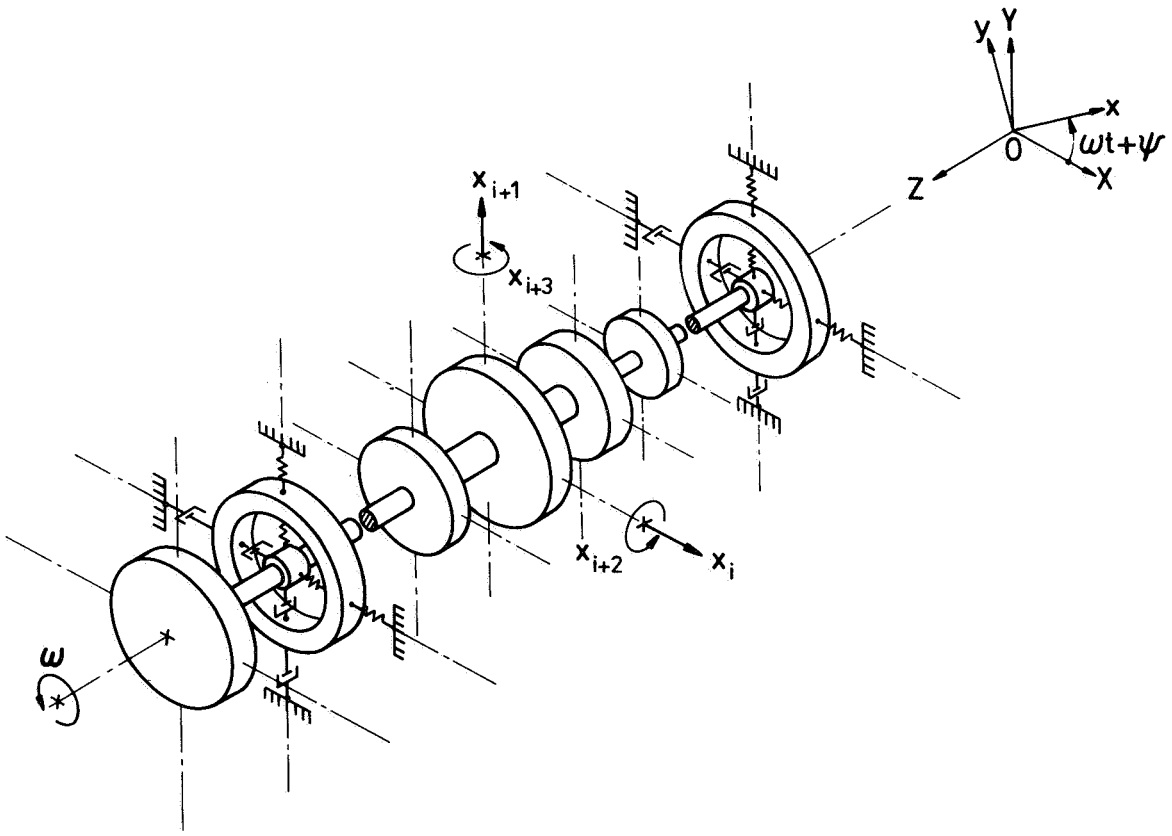

Figure 1 Typical multimass flexible rotor running in damped flexible supports

and where $$P_{S_{ij}} = \frac{\partial F_{S_i}}{\partial X_j} , \tag{7}$$

and $$Q_{S_{ij}} = \frac{\partial F_{S_i}}{\partial \dot{X}_j} . \tag{8}$$

Thus, neglecting higher order terms, equation (4) may also be written as:

$$\mathbf{M}\delta\ddot{\underline{X}} + (\mathbf{C} - \mathbf{Q}_S)\delta\dot{\underline{X}} + (\mathbf{K} - \mathbf{P}_S)\delta\underline{X} = \underline{0} . \tag{9}$$

The existence of the partial derivatives is assumed and they are evaluated at $\underline{X}_o, \dot{\underline{X}}_o$.

Unfortunately, the elements of $\mathbf{Q}_S$ and $\mathbf{P}_S$, involving derivatives of damper forces, are in general time dependent, so that equations (9) do not reduce to an eigenvalue problem. To overcome this difficulty, one may choose a rotating cartesian reference frame (x,y,Z) wherein the cartesian axis pair (x,y) rotates with angular velocity ω about the Z axis as shown in figure 1. If $\underline{x}$ be the vector of displacements in the rotating frame, then:

$$\underline{X} = \mathbf{T}\underline{x} , \tag{10}$$

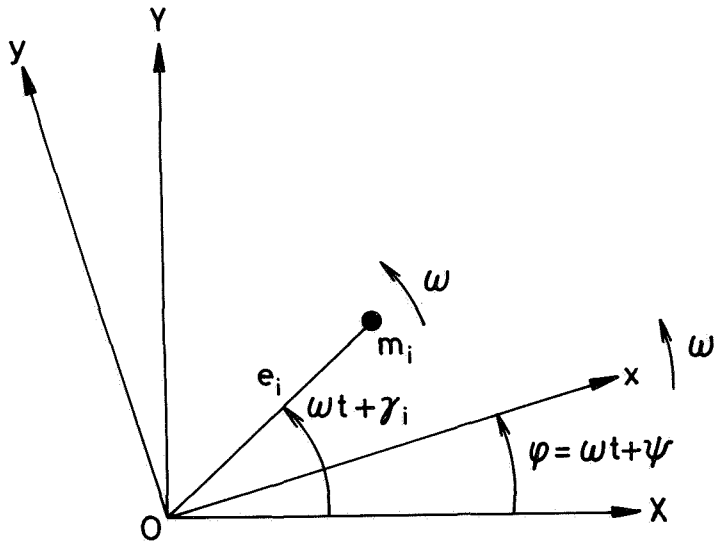

Figure 2 Location of damper mass m_i in fixed and rotating reference frames

where for an n degree of freedom system (n even), the transformation matrix $\mathbf{T}$ is given by:

$$\mathbf{T} = \begin{bmatrix} \mathbf{\Lambda} & & \mathbf{0} \\ & \ddots & \\ \mathbf{0} & & \mathbf{\Lambda} \end{bmatrix}, \tag{11}$$

with equal 2×2 diagonal submatrices $\mathbf{\Lambda}$, where:

$$\mathbf{\Lambda} = \begin{bmatrix} \cos\phi & -\sin\phi \\ \sin\phi & \cos\phi \end{bmatrix}, \tag{12}$$

and

$$\phi = \omega t + \psi \quad . \tag{13}$$

Note that ψ, the angular displacement of the xy axes from the XY axis at time t=0 is arbitrary. Premultiplying equation (1) by $\mathbf{T}^{-1}$ gives forces in the rotating frame, i.e.:

$$\mathbf{T}^{-1}(\mathbf{M}\ddot{\underline{X}} + \mathbf{C}\dot{\underline{X}} + \mathbf{K}\underline{X}) = \mathbf{T}^{-1}\underline{F}_S = \underline{F}_R \quad . \tag{14}$$

Hence, as shown in the Appendix, substitution of equation (10) into equation (14) yields:

$$\mathbf{M}\ddot{\underline{x}} + (\mathbf{C} + 2\omega\hat{\mathbf{M}})\dot{\underline{x}} + (-\omega^2\mathbf{M} + \omega\hat{\mathbf{C}} + \mathbf{K})\underline{x} = \underline{F}_R \quad . \tag{15}$$

If $\underline{x}_o$ be the steady state solutions of equation (15), then following the same arguments as above for the stationary frame, the equations of motion consequent upon system perturbation $\delta\underline{x}$, become:

$$\mathbf{M}\delta\ddot{\underline{x}} + (\mathbf{C} + 2\omega\hat{\mathbf{M}} - \mathbf{Q}_R)\delta\dot{\underline{x}} + (-\omega^2\mathbf{M} + \omega\hat{\mathbf{C}} + \mathbf{K} - \mathbf{P}_R)\delta\underline{x} = \underline{0} , \tag{16}$$

or

$$\mathbf{M}\delta\ddot{\underline{x}} + \mathbf{C}^*\delta\dot{\underline{x}} + \mathbf{K}^*\delta\underline{x} = \underline{0} , \tag{17}$$

where

$$\mathbf{C}^* = \mathbf{C} + 2\omega\hat{\mathbf{M}} - \mathbf{Q}_R , \tag{18}$$

$$\mathbf{K}^* = \mathbf{K} + \omega\hat{\mathbf{C}} - \omega^2\mathbf{M} - \mathbf{P}_R , \tag{19}$$

$$P_{R_{ij}} = \frac{\partial F_{R_i}}{\partial x_j} , \tag{20}$$

and

$$Q_{R_{ij}} = \frac{\partial F_{R_i}}{\partial \dot{x}_j} . \tag{21}$$

Again, the $P_{R_{ij}}$ and the $Q_{R_{ij}}$ are assumed to exist and are evaluated at $\underline{x}_o$. (Note that $\dot{\underline{x}}_o = \underline{0}$.)

In general, the steady state damper eccentricities e_i will have constant phase angles $(\gamma_i - \psi)$ with respect to the x axis, as shown in figure 2. Hence, the elements of $\mathbf{P}_R$ and $\mathbf{Q}_R$ will be functions of e_i and $(\gamma_i - \psi)$, where ψ is arbitrary. By selecting ψ equal to one of the γ_i's (say γ_1), $\mathbf{P}_R$ and $\mathbf{Q}_R$ will, in the general case of m dampers, be functions of $(2m - 1)$ quantities $e_1, e_2, \ldots, e_m, \gamma_2-\gamma_1, \gamma_3-\gamma_1, \ldots, \gamma_m-\gamma_1$.

Note that the coefficients of $\delta\ddot{\underline{x}}$, $\delta\dot{\underline{x}}$ and $\delta\underline{x}$ in equation (17) are constants, i.e. independent of time, so one is immediately in a position to investigate the stability and the damping pertaining to the equilibrium solutions $\underline{x}_o$ by examining the solutions of equation (17), a set of n homogeneous second order linear differential equations with constant coefficients. Thus, by assuming solutions of the form:

$$\delta\underline{x} = \underline{\chi}e^{\lambda t} , \tag{22}$$

where the $\underline{\chi}$ and λ may be complex, non-trivial solutions of equation (17) exist, if, and only if:

$$\det[\lambda^2\mathbf{M} + \lambda\mathbf{C}^* + \mathbf{K}^*] = 0 . \tag{23}$$

Equation (23), the characteristic equation of the perturbed system, is a polynomial of degree 2n in λ. The stability of, and the damping pertaining to the equilibrium solutions $\underline{x}_o$ depend on the real parts of the roots of equation (23) with the stability threshold being determined by that combination of system parameters which result in any pair of roots, $\lambda_{1,2} = \pm j\Omega$, where Ω is the natural frequency at the stability threshold. Note that one such possible stability threshold corresponding to Ω=0 (i.e. $\lambda_{1,2} = \pm j0$) will occur whenever:

$$\det[\mathbf{K}^*] = 0 . \tag{24}$$

If stability threshold determinations were the sole requirement, one could dispense with the need to find the roots $\lambda_1, \ldots, \lambda_{2n}$ and apply a linear systems theory technique, e.g. Routh's Criterion, to the coefficients of equation (23). Such was

the procedure adopted in reference 3. If the degree of damping is of interest, one needs to resort in general to some numerical procedure for finding the roots.

An alternative and numerically far more simply approach, in so far as programming effort is concerned, is to utilize generally available eigenvalue solution procedures, by recasting equations (17) into a recognizable eigenvalue problem. The normal procedure is to transform these n second order differential equations into the 2n first order equations (see for example reference 4):

$$\mathbf{A}\dot{\underline{u}} + \mathbf{B}\underline{u} = \underline{0} , \tag{25}$$

where

$$\underline{u} = \begin{bmatrix} \delta\dot{\underline{x}} \\ \delta\underline{x} \end{bmatrix} , \tag{26}$$

$$\mathbf{A} = \begin{bmatrix} \mathbf{0} & \mathbf{M} \\ \mathbf{M} & \mathbf{C}^* \end{bmatrix} , \tag{27}$$

and

$$\mathbf{B} = \begin{bmatrix} -\mathbf{M} & \mathbf{0} \\ \mathbf{0} & \mathbf{K}^* \end{bmatrix} . \tag{28}$$

By assuming solutions of the form:

$$\underline{u} = \underline{\eta} e^{\lambda t} , \tag{29}$$

where the $\underline{\eta}$ and λ may be complex, non-trivial solutions of equation (23) exist if, and only if:

$$\det[\lambda\mathbf{A} + \mathbf{B}] = 0 . \tag{30}$$

Equation (30) is a polynomial of degree 2n in λ. It is equivalent to the characteristic equation (23). The 2n values of λ, the roots of the characteristic equation, are in this formulation more commonly referred to as eigenvalues. Once the 2n eigenvalues have been located for a given choice of system parameters, both the stability and the degree of damping present can be quantified.

SYSTEM WITH ONE DAMPER

So far the problem formulation has been quite general. If one restricts attention to a single damper, an important simplification occurs if ψ is set equal to γ_1, whereupon the elements of $\mathbf{P}_R$ and $\mathbf{Q}_R$ in equations (16) are functions of e_1 only. Thus, the need to evaluate γ_1 is avoided, thereby simplifying stability evaluation and design data portrayal.

For design study purposes, it is convenient to non-dimensionalize equations (16) by dividing the force equations by $mC\omega^2$ and the moment equations by $mC^2\omega^2$ and introducing the non-dimensional time $\tau = \omega t$. The above theory is otherwise unchanged, except all quantities are now non-dimensional. In particular, one can utilize equation (24) immediately to find those stability thresholds which pertain to zero

natural frequency. Note that the non-zero elements of $\mathbf{P}_R$ are located in a 2×2 submatrix, the elements of which are products of ω_b/ω and functions of ε, where ω_b is a bearing parameter involving the bearing dimensions and lubricant viscosity. Thus, whereas equation (24) is a non-linear equation in ε, and for a given ω_b, could be solved iteratively by some appropriate technique such as the search procedure, one may note that for some assumed ε but unspecified ω_b, this equation is a quartic in ω_b when the damper is flexibly supported, and a quadratic in ω_b when the damper is rigidly supported. Hence one can determine directly from equation (24) the physically meaningful values of ω_b (if any) which satisfy it. A repetition of this for other values of ω would enable the stability thresholds corresponding to zero natural frequency and various values of ε to be drawn on a design map with ω_b as ordinate and ω as abscissa.

Note that such a map is possible regardless of the number of degrees of freedom, or of the unbalance distribution. If drawn to the same scale, it can be directly superimposed on the corresponding equilibrium orbit eccentricity design maps in reference 2, thereby indicating at a glance, the likelihood of operation in the vicinity of, or within, this particular type of unstable region. Note that the absence of other stability thresholds (at some non-zero natural frequency) has not been proven, and to be sure that all stability regions have been located, one would need to apply a more general technique, e.g. Routh's Criterion, to equation (23) over the range of $0 < \varepsilon < 1$, for the range of values of ω_b and ω of interest, a rather daunting task even for systems with only four degrees of freedom.

ILLUSTRATIVE EXAMPLE

The utility of the above approach will be illustrated for the single disc symmetric flexible rotor, previously investigated for stability in reference 3 and for which equilibrium solutions are available in reference 2.

Figure 3 is a diagram of this system with node 1 being taken at the central disc of mass $2m_1$, and nodes 2 and 3 at the ends of the rotor which are supported by identical squeeze film dampers. The lumped mass at the bearing ends is m_2, the retainer spring for central preloading has stiffness k_2 and the rotor stiffness between the central and either end node is k_1. All unbalance is assumed to be at the disc, resulting in a disc mass eccentricity ρ_1. Viscous damping at the disc is $2c_1$. Since the rotor is symmetric about the disc, it will suffice to consider one half of the system only. The equations of motion, appropriately ordered, for this system at a rotor speed ω are given by:

$$\left.\begin{aligned}
m_1\ddot{X}_1 + c_1\dot{X}_1 + k_1(X_1 - X_2) &= \rho_1 m_1\omega^2\cos(\omega t) = F_1 \\
m_1\ddot{X}_2 + c_1\dot{X}_2 + k_1(X_2 - X_4) &= \rho_1 m_1\omega^2\sin(\omega t) = F_2 \\
m_2\ddot{X}_3 + k_1(X_3 - X_1) + k_2X_3 &= F_3 \\
m_2\ddot{X}_4 + k_1(X_4 - X_2) + k_2X_4 &= F_4
\end{aligned}\right\} \qquad (31)$$

The equations of motion for the perturbed system are given by equations (16), which, in nondimensional form, upon dividing each equation by $(m_1+m_2)C\omega^2$ and letting $\tau = \omega t$, become:

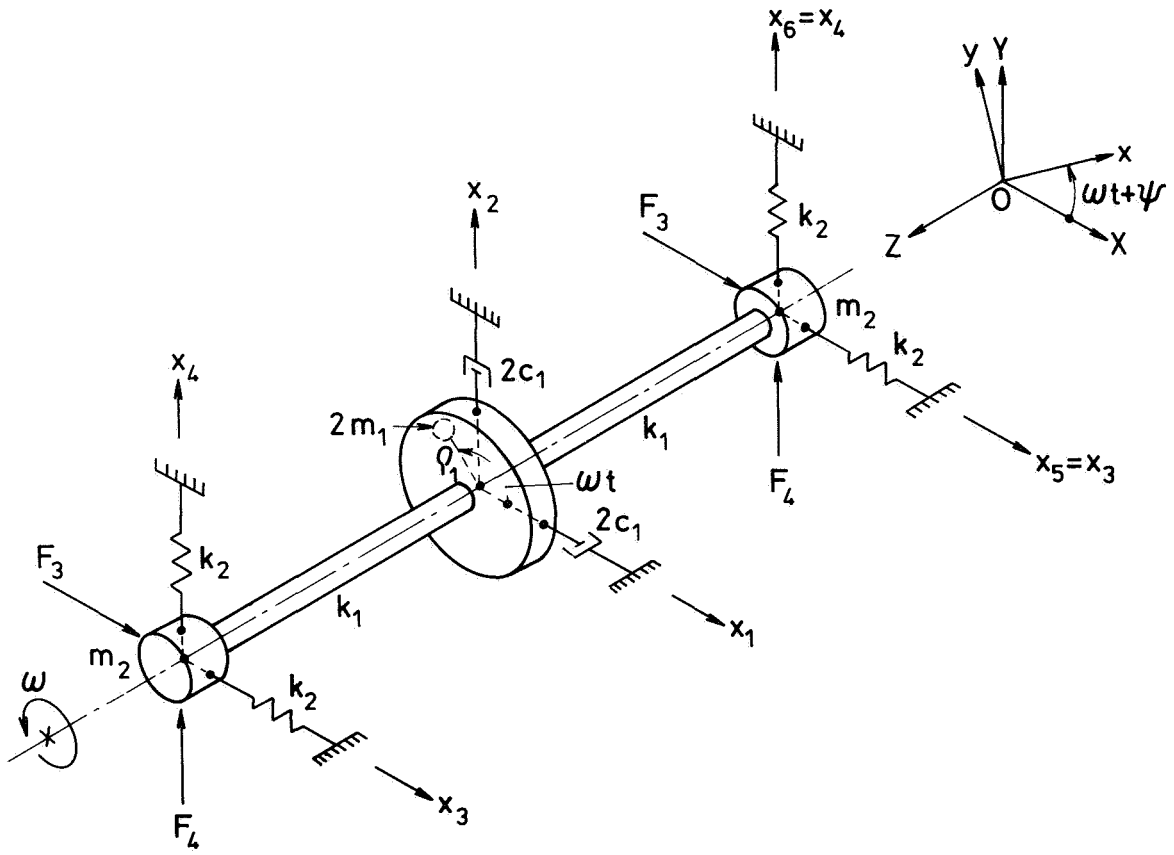

Figure 3 Flexible, symmetric unbalanced rotor supported on identical squeeze film dampers and retainer springs

$$\begin{bmatrix} M_1 & 0 & 0 & 0 \\ 0 & M_1 & 0 & 0 \\ 0 & 0 & M_2 & 0 \\ 0 & 0 & 0 & M_2 \end{bmatrix} \begin{bmatrix} \bar{x}_1'' \\ \bar{x}_2'' \\ \bar{r}'' \\ \bar{s}'' \end{bmatrix} + \begin{bmatrix} C_1 & -2M_1 & 0 & 0 \\ 2M_1 & C_1 & 0 & 0 \\ 0 & 0 & -\omega_b C_{rr}/\omega & -\omega_b C_{rs}/\omega - 2M_2 \\ 0 & 0 & -\omega_b C_{sr}/\omega + 2M_2 & -\omega_b C_{ss}/\omega \end{bmatrix} \begin{bmatrix} \bar{x}_1' \\ \bar{x}_2' \\ \bar{r}' \\ \bar{s}' \end{bmatrix}$$

$$+ \begin{bmatrix} K_1-M_1 & -C_1 & -K_1 & 0 \\ C_1 & K_1-M_1 & 0 & -K_1 \\ -K_1 & 0 & K_1+K_2-M_2-\omega_b K_{rr}/\omega & -\omega_b K_{rs}/\omega \\ 0 & -K_1 & -\omega_b K_{sr}/\omega & K_1+K_2-M_2-\omega_b K_{ss}/\omega \end{bmatrix} \begin{bmatrix} \bar{x}_1 \\ \bar{x}_2 \\ \bar{r} \\ \bar{s} \end{bmatrix} = \underline{0} \quad , \qquad (32)$$

where, to simplify the notation, the damper degrees of freedom x_3 and x_4 are denoted by r and s respectively. The coefficients K_{rr}, C_{rr}, ..., etc. are available in analytical form for unpressurized and fully pressurized (π and 2π film) dampers for both the short (Ocvirk) and finite width (Warner) bearing approximations (ref. 5). Thus, for the unpressurized or fully pressurized bearings respectively, and using the

short bearing approximation, one has:

$$K_{rr} = -\frac{4\varepsilon(1+\varepsilon^2)}{(1-\varepsilon^2)^3} \quad \text{or} \quad 0 \ , \tag{33}$$

$$K_{rs} = -C_{ss} = \frac{\pi}{2(1-\varepsilon^2)^{3/2}} \quad \text{or} \quad \frac{\pi}{(1-\varepsilon^2)^{3/2}} \ , \tag{34}$$

$$K_{sr} = C_{rr} = \frac{-\pi(1+2\varepsilon^2)}{2(1-\varepsilon^2)^{5/2}} \quad \text{or} \quad \frac{-\pi(1-2\varepsilon^2)}{(1-\varepsilon^2)^{5/2}} \ , \tag{35}$$

and

$$K_{ss} = C_{rs} = C_{sr} = \frac{-2\varepsilon}{(1-\varepsilon^2)^2} \quad \text{or} \quad 0 \ . \tag{36}$$

The equation obtained by setting the determinant of $\mathbf{K}^*$ in equation (32) equal to zero is a quadratic in ω_b, and may be solved for given values of ε and ω.

To present the data in terms of non-dimensional quantities, it is convenient to plot a non-dimensional bearing parameter ω_b/ω_c against the non-dimensional rotor speed ω/ω_c, where ω_c is some characteristic natural frequency of the system, say, the highest undamped natural frequency of the system which will fall below the desired operating speed. Equation (24) was then solved for ω_b/ω_c over a range of ω/ω_c and ε to obtain the zero natural frequency stability threshold maps if figure 4, using the following values of the non-dimensional system parameters:

$$M_2 = 0.25 \ ,$$

$$M_1 = 1 - M_2 = 0.75 \ ,$$

$$K_1 = (1 - M_2')/(\omega/\omega_c)^2 = 0.75(\omega/\omega_c)^2 \ ,$$

$$K_2 = (\omega_r/\omega_c)^2/(\omega/\omega_c)^2 = 0.25(\omega/\omega_c)^2 \ ,$$

$$C_1 = 2\zeta(1 - M_2)/(\omega/\omega_c) = 0.0075/(\omega/\omega_c) \ .$$

The quantities ω_r, ω_c and ζ are defined in the notation. (Using the notation in reference 3, the above choice of parameters would correspond to $\alpha = 0.25$, $f = 0.5$, $\zeta = 0.0005$, $a = \omega/\omega_c$ and $B = \omega_b/\omega_c$.) Here, ω_c is the first pin-pin critical speed of the rotor.

Note that provided the same scales are used for the axes ω_b/ω_c and ω/ω_c, one can overlay this stability threshold map not only over the equilibrium eccentricity orbit map given in figure 3 in reference 2 which is for an unbalance parameter $U = 0.3$, but also over any such map for the system, regardless of the unbalance distribution. These zero frequency stability thresholds were compared to the stability thresholds for $\omega_b/\omega_c = 0.1$, 0.3, 0.6 and 1.0 in figure 8 of reference 3, which were determined using Routh's Criterion. No stability thresholds were found for $\varepsilon \leqslant 0.61$. For $\omega/\omega_c \leqslant 1$ there is agreement. However, for $\omega/\omega_c > 1$, the predicted regions of instability in figure 8 of reference 3 exceed those of figure 4. Thus, figure 4 does not provide full stability threshold information; and for this, one would need to resort to an approach such as Routh's Criterion.

As an alternative or in addition to seeking stability thresholds, and to determine the degree of damping pertaining to the equilibrium solutions, one can find the eigenvalues λ_i for the system in figure 3 by forming equation (25) and using an

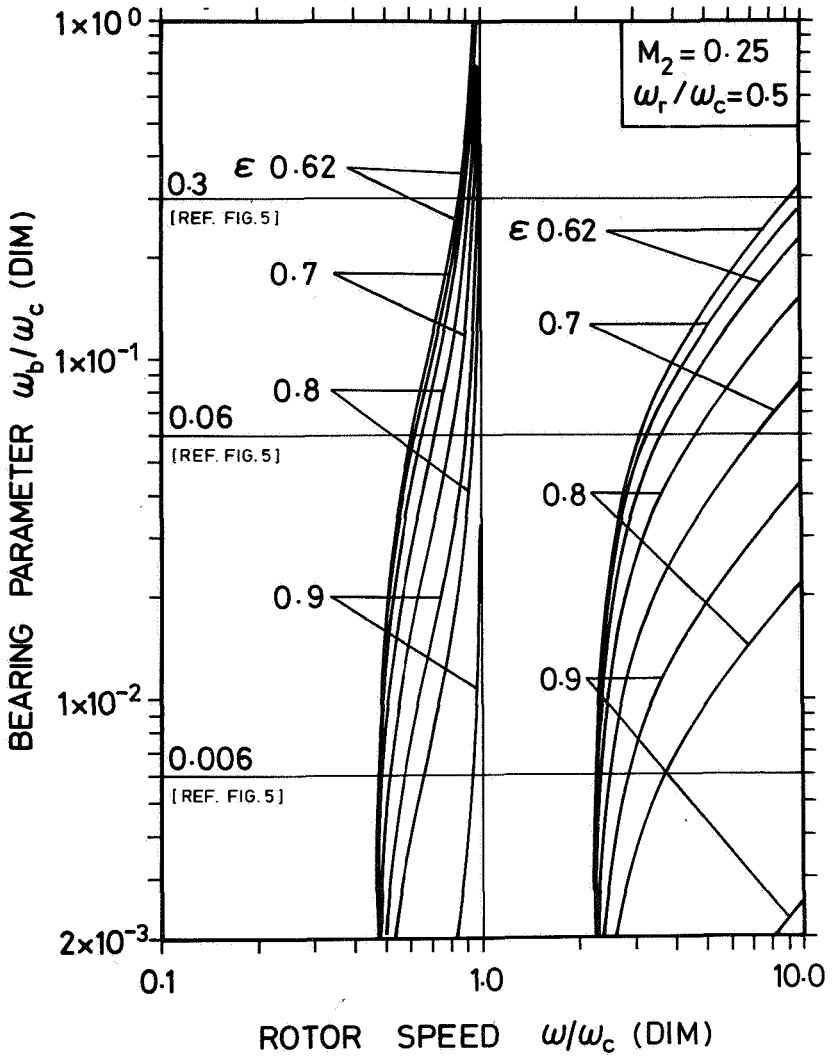

Figure 4 Zero natural frequency stability map for the system in figure 3

eigenvalue solver to determine the λ_i (i =1, 2, ..., 8). This was done for the particular equilibrium solutions indicated on figure 5 (corresponding to figure 4 in reference 2). If any of the λ_i have non-negative real parts, the solution is regarded as unstable. Where all the λ_i have negative real parts the solution is stable. Of particular interest is the degree of relative damping present in such stable solutions, particularly in the low orbit eccentricity solution when multiple solutions are possible, as this gives a qualitative indication of the likelihood of jumping to the undesirable and possibly unstable high orbit solution upon some system perturbation. Various means of determining this relative damping are available (ref.4) such as the smallest logarithmic decrement, $-2\pi Re(\lambda)/|Im(\lambda)|$, or the smallest damping ratio, $-Re(\lambda)/|\lambda|$. Either of these quantities requires the determination of the λ_i. The latter quantity is indicated for illustrative purposes in figure 5. For example, at ω/ω_c =0.3, the damping ratios corresponding to ω_b/ω_c =0.006, 0.06 and 0.3 are 0.0053, 0.047 and 0.23 respectively. The equilibrium solution for ω_b/ω_c =0.3 could

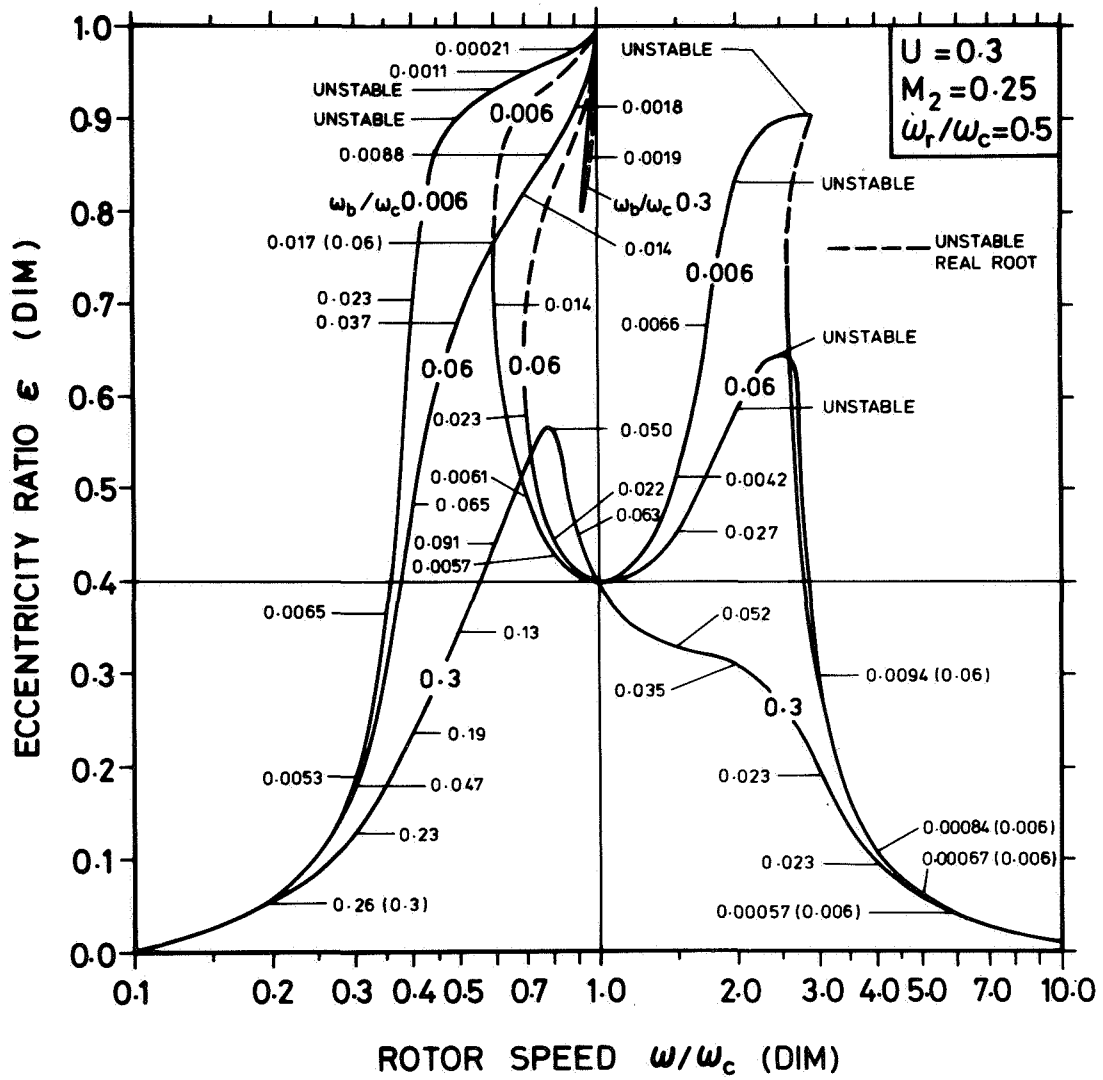

Figure 5 Damping ratios at selected points on the rotor response curves for various values of bearing parameter for the system in figure 3

be regarded as having a high degree of relative damping whereas that for $\omega_b/\omega_c = 0.006$ could be regarded as having a low degree of relative damping.

Wherever multiple solution possibilities exist, all intermediate solutions were unstable. In all such cases, the oscillation frequency was zero, and the instability was predicted by the stability map of figure 4. However, unstable single solutions are also indicated, as well as unstable higher eccentricity solutions in case of multiple solutions. In such cases the introduction of the damper has worsened system behaviour. Such unexpected unstable solutions occurred for ω_b/ω_c equal to 0.006 and 0.06 but not for 0.3. In all such cases, the oscillation frequency was always non-zero and was not predicted by the zero frequency stability map of figure 4.

This provides additional proof that figure 4 does not provide full stability threshold information. The number of equilibrium solutions investigated for instability proved insufficient to yield definitive trends in the variation of relative damping as one progresses along any particular frequency response curve in figure 5. To pick up such trends, a more thorough investigation of the λ_i would need to be undertaken. This is not warranted, for the purpose of this example was not to investigate in detail the particular system of figure 3, but rather to illustrate how simply the technique developed in the paper may be put to practical use.

Note that although figure 4 does not represent global stability thresholds, it does predict the instability of all the "intermediate" solutions and so, it serves as a locator of jump speeds, i.e. speeds at which there is a transition from a speed for which there is only one solution to one where there are at most two stable solutions or vice versa. Since the high orbit eccentricity solution, if stable, is still undesirable, generally resulting in unbalance force magnification, operation in the vicinity of such jump speed regions should be avoided. Though only proven for the model in figure 3, this equivalence between the zero frequency stability map and jump speed location is expected to be valid for general multi-degree of freedom systems. If so, a relatively simple way has been found for delineating multistable operation possibilities for any system with one damper.

CONCLUSIONS

1. A technique is developed for investigating the stability of and the degree of damping in the circular synchronous orbit solutions of n degree of freedom rotor bearing systems. In general, the technique requires finding the 2n eigenvalues of the linearized perturbation equations.

2. The perturbation equations of motion are not a function of the unbalance distribution, so for a given system a single global stability map suffices for all unbalance distributions of interest.

3. Zero-frequency stability thresholds may be found by solving as many simultaneous non-linear equations as there are dampers. If the system contains one damper only, all such stability thresholds may be found directly by solving at most a quartic equation.

4. Zero-frequency stability maps do not provide full stability information, but for the four degree of freedom system investigated in the illustrative example, and probably for more general higher degree of freedom systems as well, such maps provide a simple way to delineate multiple solution possibilities.

5. Depending on the system parameters, single equilibrium and, where multiple equilibrium solution possibilities exist, the high orbit eccentricity solution may also be unstable, with the likelihood of instability apparently increasing as the bearing parameter is reduced. Thus, the introduction of an unpressurized squeeze film damper may promote instability in an otherwise stable system.

REFERENCES

1. Greenhill, L.M. and Nelson, H.D.: Iterative Determination of Squeeze Film Damper Eccentricity for Flexible Rotor Systems. ASME Journal of Mechanical Design, vol. 104, no. 2, 1982, pp. 334-338.

2. McLean, L.J. and Hahn, E.J.: Unbalance Behaviour of Squeeze Film Damped Multi-Mass Flexible Rotor Bearing Systems. ASME Journal of Lubrication Technology, vol. 105, no. 1, 1983, pp. 22-28.

3. Rabinowitz, M.D. and Hahn, E.J.: Stability of Squeeze Film Damper Supported Flexible Rotors. ASME Journal of Engineering for Power, vol. 99, no. 4, 1977, pp. 545-551.

4. Tse, F.S., et al: Mechanical Vibrations, 2nd ed., Allyn and Bacon, Inc., Boston, 1978.

5. Hahn, E.J.: Stability and Unbalance Response of Centrally Preloaded Rotors Mounted in Journal and Squeeze Film Bearings. ASME Journal of Lubrication Technology, vol. 101, no. 2, 1979, pp. 120-128.

6. Nelson, H.D.: A Finite Rotating Shaft Element Using Timoshenko Beam Theory. ASME Journal of Mechanical Design, vol. 102, no. 4, 1980, pp. 793-803.

APPENDIX

Since

$$\underline{X} = \mathbf{T}\underline{x} \quad , \tag{A1}$$

$$\dot{\underline{X}} = \dot{\mathbf{T}}\underline{x} + \mathbf{T}\dot{\underline{x}} \quad , \tag{A2}$$

$$\ddot{\underline{X}} = \ddot{\mathbf{T}}\underline{x} + 2\dot{\mathbf{T}}\dot{\underline{x}} + \mathbf{T}\ddot{\underline{x}} \quad , \tag{A3}$$

where

$$\dot{\mathbf{T}} = \omega \begin{bmatrix} \mathbf{\Lambda}^* & & \mathbf{0} \\ & \ddots & \\ \mathbf{0} & & \mathbf{\Lambda}^* \end{bmatrix} \quad , \tag{A4}$$

and

$$\mathbf{\Lambda}^* = \begin{bmatrix} -\sin\phi & -\cos\phi \\ \cos\phi & -\sin\phi \end{bmatrix} \quad , \tag{A5}$$

it follows that

$$\dot{\mathbf{T}} = \omega \mathbf{T}^* \quad , \tag{A6}$$

and

$$\ddot{\mathbf{T}} = -\omega^2 \mathbf{T} \quad . \tag{A7}$$

Hence, substitution of equation (10) into equation (14) gives:

$$\mathbf{T}^{-1}\mathbf{M}\mathbf{T}\ddot{\underline{x}} + (2\omega\mathbf{T}^{-1}\mathbf{M}\mathbf{T}^{*} + \mathbf{T}^{-1}\mathbf{C}\mathbf{T})\dot{\underline{x}} + (\omega\mathbf{T}^{-1}\mathbf{C}\mathbf{T}^{*} + \mathbf{T}^{-1}\mathbf{K}\mathbf{T} - \omega^{2}\mathbf{T}^{-1}\mathbf{M}\mathbf{T})\underline{x} = \underline{F}_{R} \quad , \tag{A8}$$

where
$$\mathbf{T}^{-1} = \begin{bmatrix} \mathbf{\Lambda}^{-1} & \cdots & \mathbf{0} \\ \vdots & \ddots & \vdots \\ \mathbf{0} & \cdots & \mathbf{\Lambda}^{-1} \end{bmatrix} \quad , \tag{A9}$$

and
$$\mathbf{\Lambda}^{-1} = \begin{bmatrix} \cos\phi & \sin\phi \\ -\sin\phi & \cos\phi \end{bmatrix} \quad . \tag{A10}$$

To evaluate $\mathbf{T}^{-1}\mathbf{M}\mathbf{T}$, it is convenient to partition it into 2×2 submatrices. Any one of these submatrices will have the form $\mathbf{\Lambda}^{-1}\mathbf{m}\mathbf{\Lambda}$, where $\mathbf{m}$ is the corresponding submatrix of $\mathbf{M}$. Then it is easy to show that $\mathbf{\Lambda}^{-1}\mathbf{m}\mathbf{\Lambda}$ equals $\mathbf{m}$, if, and only if, the elements of $\mathbf{m}$ are of the form:

$$\mathbf{m} = \begin{bmatrix} m_1 & -m_2 \\ m_2 & m_1 \end{bmatrix} \quad . \tag{A11}$$

Hence, if equation (A11) is satisfied for all submatrices of $\mathbf{M}$, then $\mathbf{T}^{-1}\mathbf{M}\mathbf{T}$ equals $\mathbf{M}$. Conditions similar to equation (A11) are required for $\mathbf{T}^{-1}\mathbf{C}\mathbf{T}$ and $\mathbf{T}^{-1}\mathbf{K}\mathbf{T}$ to equal $\mathbf{C}$ and $\mathbf{K}$ respectively. As may be seen from reference 6, such conditions are satisfied for $\mathbf{M}$, $\mathbf{C}$ and $\mathbf{K}$ matrices in general, even when gyroscopic effects are present.

To evaluate $\mathbf{T}^{-1}\mathbf{M}\mathbf{T}^{*}$, it is again convenient to partition it into 2×2 submatrices. Any one of these submatrices will have the form $\mathbf{\Lambda}^{-1}\mathbf{m}\mathbf{\Lambda}^{*}$, where $\mathbf{m}$ is the corresponding submatrix of $\mathbf{M}$. Hence, noting that $\mathbf{m}$ will be of the form given by equation (A11), $\mathbf{\Lambda}^{-1}\mathbf{m}\mathbf{\Lambda}^{*}$ will equal $\hat{\mathbf{m}}$ where $\hat{\mathbf{m}}$ is given by:

$$\hat{\mathbf{m}} = \begin{bmatrix} -m_2 & -m_1 \\ m_1 & -m_2 \end{bmatrix} \tag{A12}$$

Thus $\mathbf{T}^{-1}\mathbf{M}\mathbf{T}^{*}$ equals $\hat{\mathbf{M}}$, where the 2×2 submatrices $\hat{\mathbf{m}}$ of $\hat{\mathbf{M}}$ are formed from the corresponding submatrices $\mathbf{m}$ of $\mathbf{M}$ according to equations (A11) and (A12). Similarly $\mathbf{T}^{-1}\mathbf{C}\mathbf{T}^{*}$ equals $\hat{\mathbf{C}}$. Hence, equation (A8) simplifies to:

$$\mathbf{M}\ddot{\underline{x}} + (2\omega\hat{\mathbf{M}} + \mathbf{C})\dot{\underline{x}} + (-\omega^{2}\mathbf{M} + \omega\hat{\mathbf{C}} + \mathbf{K})\underline{x} = \underline{F}_{R} \quad . \tag{A13}$$

Equation (A13) is the equation of motion in the rotating frame. Note that the coefficients of $\underline{x}$, $\dot{\underline{x}}$ and $\ddot{\underline{x}}$ are all constants.